iomac
International Operational Modal Analysis Conference

11th International Operational Modal Analysis Conference

20 - 23 May 2025 | Rennes, France

Design optimisation of lightweight aerospace structures for vibration fatigue

Stefan Anderson [1], *Jonathan Cooper* [2], *Fabrizio Scarpa* [3], *and Brano Titurus* [4]

[1] University of Bristol, sa14378@bristol.ac.uk
[2] University of Bristol, j.e.cooper@bristol.ac.uk
[3] University of Bristol, f.scarpa@bristol.ac.uk
[4] University of Bristol, brano.titurus@bristol.ac.uk

ABSTRACT

A methodology is developed for optimising the design of simple lightweight structures, such as those found attached to aircraft wings, which experience excitation over a wide frequency range at intermediate frequencies and above. The optimisation focuses on ensuring that constraints on fatigue damage are satisfied whilst weight is reduced; an understanding is gained of the design space presented by these structures. Small-scale structures are employed to model plate fairing surrogates, first in isolation and then attached to a flexible beam. The plates undergo synthetic random fatigue loading using Finite Element analyses with Fatigue Damage then computed in the frequency domain using the Dirlik method. The modal behaviour is compared, and the effect of the addition of semicircular notches is assessed. The design space presented by a plate where the thicknesses of different regions are allowed to vary is found to be non-smooth and irregular, motivating a global optimisation approach. Finally, a global optimisation of a system of two plates attached to a flexible beam is performed. Qualitative and quantitative comparisons between the optimal fairing designs obtained under this optimisation are made. The global optimization is found to perform well in cases where low-frequency excitation is present, but provides no design improvement over local optimisation in cases which exclusively contain higher frequencies.

Keywords: Lightweight Structures, Fatigue, Ambient Excitation, Modal Analysis

1. INTRODUCTION

In modern aerospace design, minimising the structural weight subject to stress, deflections and flutter constraints is crucial to achieving both performance and durability. However, lightweight structures can

be susceptible to vibration-induced fatigue in highly loaded environments such as those encountered on wings and control surfaces, but with careful dynamic design and optimisation, these structures can experience an enhanced fatigue life which can further increase the overall reliability of modern aircraft.

Fatigue damage analysis has developed significantly since the first development of S-N curves and the Palmgren-Miner rule [1], [2]. In particular, the introduction of cycle counting algorithms such as rainflow cycle counting [3] has allowed extensive simulation of fatigue in the time domain while spectral moments methods have offered a fast frequency domain alternative, e.g., [4] and [5]. Further, the development of finite element (FE) modelling led to more sophisticated models which enabled fatigue optimisation, [6], [7], [8]. For example, Liu et al. [9] used Gaussian process regression to estimate fatigue damage of floating wind turbines at a variety of sea states. In an aerospace context, formal optimisation is typically based on strength and deflection criteria rather than fatigue. However, Grobvic et al. [10] investigated wing spars using the extended finite element method and the fatigue life of the spars with different cross-sections, but constant area, was compared and an optimal spar cross-section was obtained. In that work, the loading was applied at a single frequency and the focus was on crack propagation. This type of loading is generally common across other fatigue optimisation examples.

One category of aerospace structures prone to fatigue effects consists of the various lightweight components which are placed along the wingspan. Examples of these components include panels, covers and external hardpoints. They offer a unique environment with complex interactions involving spectrally rich pressure loading and modal coupling originating due to wing flexibility interacting with a complex airflow. If these factors are accounted for during the design stage, those components may be optimised for fatigue life improvement. Analysis of existing dynamic flight test data suggests that careful consideration of the relationships between the modal characteristics of the components and the aerodynamic loading can constitute the basis for rational design improvements. Hence, a formal optimal design process driven by modal and spectral considerations can help mitigate the risks arising from reduced fatigue life.

This work explores an approach to optimise the design of lightweight structures from a fatigue point of view. A representative beam-plate benchmark problem that displays some of the configurational characteristics observed in aircraft context is used to provide an assembly where the two nominally identical lightweight components are located and coupled via a single flexible support structure. This system is loaded using a simplified spectral loading and the fatigue-sensitive design factors of individual and assembled components are studied in the frequency domain. Modal responses and damage measures are observed under various design and load changes. Additionally, optimisation of the components' subdomain thickness parameters is used to define the required design differences between the two nominally identical and elastically coupled components to achieve improved fatigue performance.

2. METHODS

2.1. Problem formulation

A small test case is introduced to investigate the effect of simplified spectral loading on fatigue damage of nominally identical lightweight components. These types of structures are typically placed along aircraft wings and tend to experience strong variable aerodynamic loading. Flight and ground vibration tests had previously indicated that such structures can experience rich multi-modal excitation. A conceptual sketch of the chosen test case is shown in figure1.

Two identical lightweight structures are modelled as 60 mm by 300 mm rectangular plates with an initial thickness of 3 mm which are then attached to a 1 m long cantilever beam with a hollow rectangular cross-section with outer dimensions of 60 mm by 15 mm and inner dimensions of 50 mm by 5 mm. The spacing between the plates is used to introduce elastic coupling with the support beam structure. All components are assumed to be made of 6061 T6 aluminium.

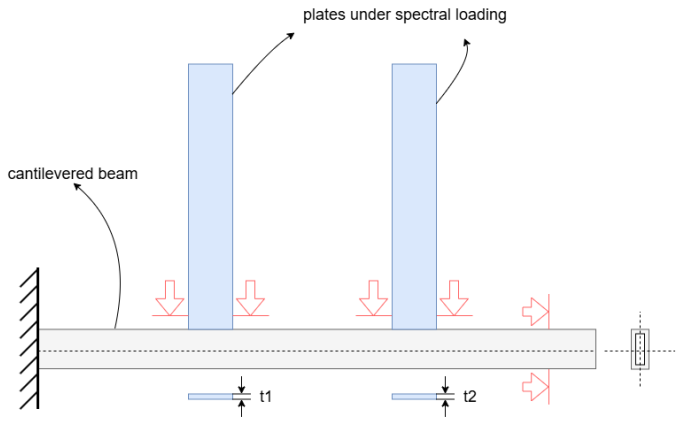

Figure 1: Problem setup for the two-plate test case. Initial plate thicknesses labelled, drawing not to scale.

2.2. FE model of the structure

The FE model was developed using the Patran/Nastran suite. Plates were initially modelled as rectangular structures. However, optimisations were performed on plates with semi-circular notches near the base (see section 3.1.. Each prismatic plate was modelled as a shell structure. Rectangular plates used 720 QUAD4 quadrilaterals, generated by Patran's Isomesh mapped mesh using mesh seeds. Notched plates were modelled using a similar mesh consisting of 677 QUAD4 and 7 TRIA elements with Patran's hybrid meshing tool. When modelled in isolation, the plates were fixed at one of their short edges. The beam fixed at one of its end points was modelled using 200 PBEAM elements with the rectangular cross-section defined above. When assembled, the plates' short edge nodes were directly attached (merged) with the corresponding beam nodes.

To mimic a typical flight environment for the lightweight components, a broadband forcing with constant power spectral density between defined frequencies was assumed. When observed in in-flight measured strain gauge data, typically several active vibration modes are excited. These can include modes at intermediate frequencies, with behaviour corresponding to up to the 9th mode identified in ground vibration tests of the components. To maintain spatial simplicity of this exploratory test case, the plates were only excited at a single node at the top left corner of each plate. In Nastran, this approach is defined as a unit load over a frequency band which evaluates relevant stress mode shapes. These are then used by the Dirlik method along with the specified P.S.D. frequency content to evaluate fatigue. In practice, the forcing function would not only be a function of aerodynamic turbulence, modelled for instance by the Von Karman Gust Spectrum [11], but also the frequency content from any separated flows (buffet) impinging upon the component.

2.3. Frequency domain fatigue and damage analysis

This project employs MSC Nastran's embedded CAE Fatigue frequency module provided by Hexagon AB [12] The damage responses are calculated in Nastran 2024.2. Optimisation study is performed using Nastran SOL 200 solver with the IPOPT algorithm. Post-processing is performed using the Engineering Lab SOL 200 web application developed by Christian Aparicio [13]. The material used in this study is 6061 T6 aluminium. Its material properties and SN data are adopted from [14]. The strain measurements observed in the past in-flight tests guide the choice of the adopted synthetic loading spectrum profile in terms of the number of vibration modes activated by the loading. Specifically, the flat spectrum is assumed which spans across the range which includes up to the first nine vibration modes of the panel components. This provides a good starting point for improving the process. In flight excitation is more concentrated around specific frequencies, which are particular to a specific geometry and flight condition. The analysis is performed in the frequency domain using Nastran's SOL 111 direct frequency response solver.

Finally, the cycle counting and the damage calculation are performed with the help of the Dirlik method in the frequency domain. The Dirlik method is a semi-empirical technique that estimates the probability density function (PDF) of stress (or strain) ranges within a random vibration environment [5]. The method further uses Miner's rule and information from the S-N curve to evaluate the fatigue damage experienced by a structure. This technique is commonly used nowadays in industry.

To apply the method for this project, a harmonic unit load was applied in frequency increments of 2.5 Hz up to 150 Hz. The stresses from these frequency responses were then used to apply P.S.D in the range 0-70 Hz using the Dirlik method. Stress combination was performed using the signed Von Mises approach and calculated at element centres. A stress-based S-N curve was used with a Neuber plasticity correction. Since the signal was generated synthetically, a mean stress correction was not required.

2.4. Optimization problem formulation

The optimisation problem is locally parameterised using the plate thickness. To initially restrict the dimensionality of the problem, the meshed plates are divided into three and, later, ten subregions. The location of these regions is informed by an initial view of the stress and fatigue distribution patterns when the plates have a constant thickness. To simulate the design problem, the total weight of the structure was optimised by varying the chosen parameters. Hence, the cost function was defined to be the total weight of the plate. The thickness of each region was constrained between 1 and 5 mm. Optimization was further constrained so that the total damage from a one second long loading cycle did not exceed 0.1% in any of the plate's regions. The loading was defined using a constant PSD which included the frequencies of the first nine modes of the plate. The magnitude of the PSD was adjusted such that the component had a life of at least 1000 cycles. A low value was chosen to ensure that an initial design was feasible with an initial thickness of 3mm.

The objective function to be minimised is therefore defined as

$$J(\mathbf{p}) = \rho\left(A^T\,\mathbf{t}\right) \text{ where } \quad \mathbf{t}_L \leq \mathbf{t} \leq \mathbf{t}_U$$

while the constraints are specified as

$$\forall e \in P_1, \quad D_e = \int_0^\infty P_e(f)\cdot g(f)\,df \leq 0.0002, \qquad \forall e \in P_2, \quad D_e = \int_0^\infty P_e(f)\cdot g(f)\,df \leq 0.0002$$

where A is the vector of the fixed subdomain areas and t is the vector of the thickness parameters, ρ is a density. In the constraint expression, for every element in plates P_1 and P_2, fatigue calculated by applying the Dirlik method $g(f)$ to the power spectral density $P_e(f)$, damage must be below the threshold value.

Local optimisation was performed using the IPOPT algorithm included within Nastran's SOL200 system. The IPOPT algorithm uses an interior point line search filter method and the implementation used in this case is described by Wachter and Bieger [15]. Evaluation of different initial conditions revealed that the local optimiser tended to converge to different optima. To address this problem, a Latin hypercube of 400 initial solutions was generated and the local IPOPT optimiser was run with restarts. Of these, the best resulting design was selected. In addition to this, a parameter study of a single notched plate with only two varying thickness parameters was performed to obtain additional insight into the design space.

3. RESULTS

This section details the results of the study of the lightweight structures under the band-limited high-cycle fatigue loading. Section 3.1. describes the reference modal behaviour in isolation and when assembled. Section 3.2. describes a parametric study of the design space for an isolated notched plate. Finally, section 3.3. presents the results of the optimisation study of a system consisting of two notched plates attached to the beam.

3.1. Reference modal analysis

The first nine modes for both a rectangular and a notched plate are shown in figure 2. The set contains five transversal bending modes, three torsion modes and an in-plane bending (shear) mode. The modes are labelled and ordered as follows: the rectangular plate modes are B1, B2, T1 B3, S1, T2, B4, T3, B5; the notched plate modes are B1, B2, S1, T1, B3, B4, T2, B5, T3. In both cases, the modes cover frequencies up to 50 Hz. To reach a more complete appreciation of the modal characteristics, both the displacement and the stress modal patterns are shown as heat maps.

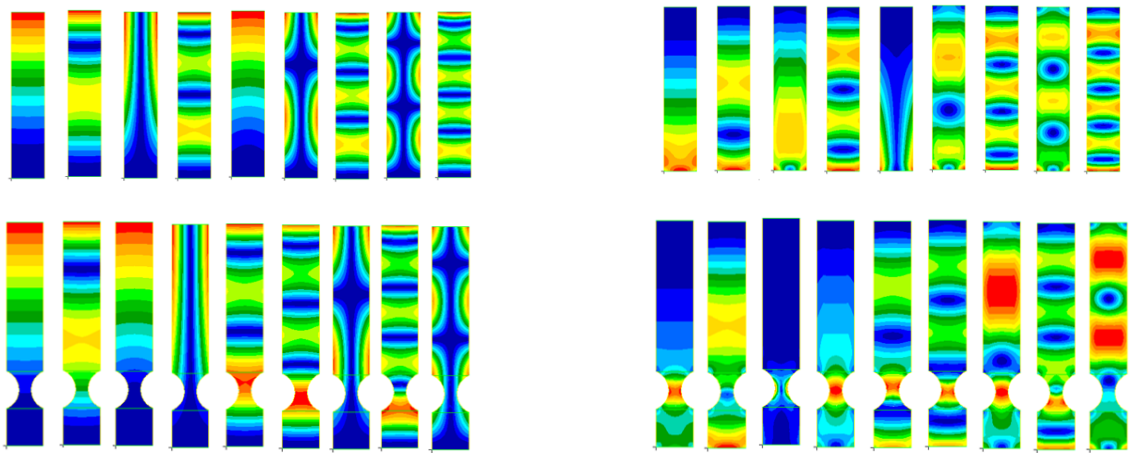

Figure 2: Displacement (left) and stress (right) modal patterns for the first 9 mode shapes of a 3 mm aluminium plate with a rectangular (top row) and notched (bottom row) profile

The modal stress patterns (right side of figure 2) reveal the stress concentration regions. Classically, these tend to be associated with the interface and transition locations such as the constrained bottom edge or the notch. The results suggest that whereas the localised thickness optimisation of the rectangular samples would likely recommend thickening near its base, a notched sample presented a more complex trade-off between the regional thicknesses.

The assembled system requires the inclusion of the first 30 modes to cover the frequency range of interest up to 50 Hz. Some examples of these mode shapes are shown in figure 3. The increased number of modes is observed because of the presence of the two nominally identical components interacting via a flexible structure. Modes 2 and 10 are examples of this behaviour. The configuration consisting of the notched plates requires up to 33 modes for the same reason, and the resulting frequency range which incorporates the modes of interest reaches 61.5 Hz.

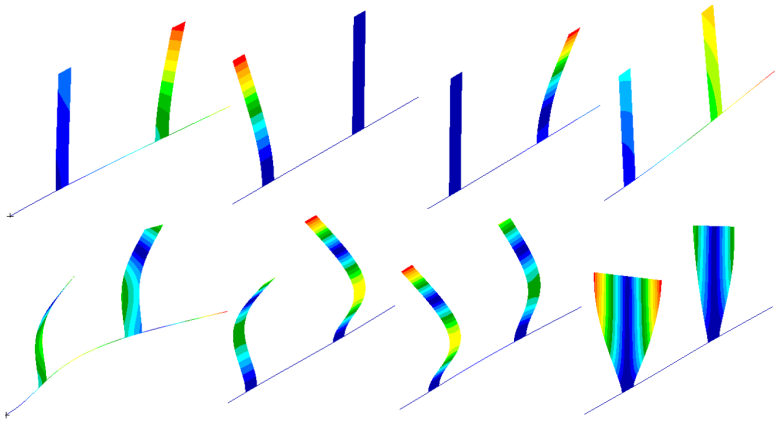

Figure 3: Plot of displacement for the first eight mode shapes of the assembled system with rectangular plates.

3.2. Parametric study

As shown in the previous section, a more complex specimen featuring a pair of semi-circular notches introduces a more complex stress concentration context. Such a case has been classically studied in other research works with a similar focus, e.g., Slavic et al. [16]. The FE model of this specimen is shown in figure 4. A point load is applied at the end of the specimen for the range 1 to 75 Hz. A point load allows for more variation in the stress field than a distributed load, easing the peak counting using the Dirlik method. The specimen is loaded at the left-hand corner, as initial analysis had shown that a more eccentric load leads to a greater proportion of fatigue occurring at higher frequencies, resulting in a richer response.

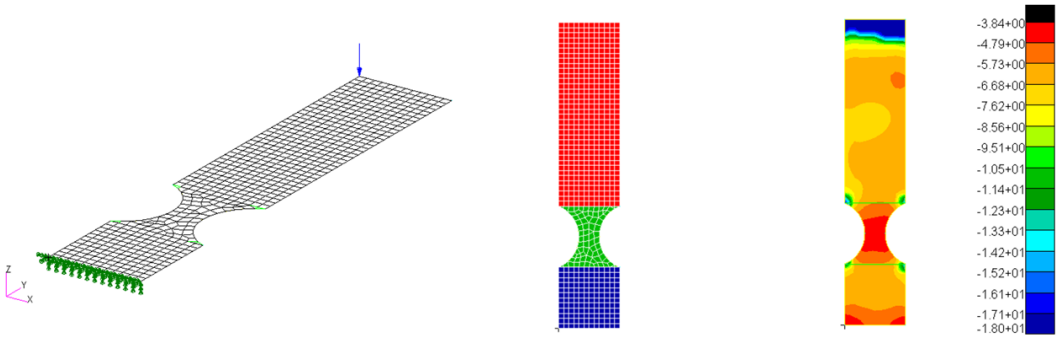

Figure 4: Initial test case used for optimisation. A load is applied at the far corner from where the plate is clamped (left). The plate is divided into three sections with different thicknesses (centre). Those highlighted in green (the notch section) and blue (the base section) are allowed to vary. The logarithm of fatigue damage under loading in the range 1 to 75 Hz is shown as a contour plot (right).

The notch narrows the sample to one-third of the nominal width of the plate at its narrowest point. The fatigue damage profile produced by exciting this sample evenly from 1 to 75 Hz is shown in figure 4. Here, high damage is indicated both at the base of the plate and also at the centre of the notch. Hence, it presents a more complex design problem. To study this case, the plate is divided into three regions. The two regions of interest are indicated in figure 4. The parts of the FE mesh shown in green (the notched section) and blue (the base section), were allowed to vary in thickness, while the red outboard section had its thickness fixed at 3 mm. To investigate the thickness impact on fatigue damage, the thicknesses of both sections were changed in increments of 0.5 mm from 1 mm to 10 mm. The fatigue analysis for each of the 361 designs was completed and the maximum fatigue damage in the structure was recorded. The results of this study are summarised in figure 5. Uniform modal critical damping of 4% is used across the frequency range. Without this, many designs experience damage over 100% over 1 second.

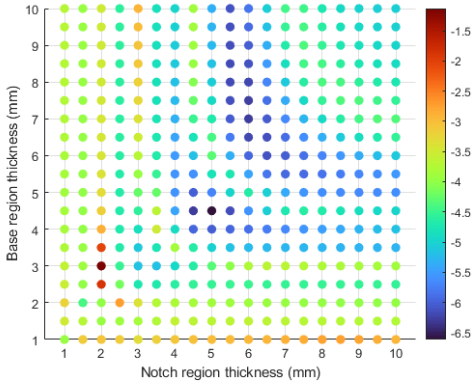

Figure 5: Log of maximum fatigue damage for designs with different thicknesses for notched and base region.

The study shows that the lowest damage is achieved with a notched region with a thickness of 5 mm and a base region with a thickness of 4.5 mm which resulted in damage of $10^{-6.6}$. It also shows a

general trend of increasing thickness, particularly increasing the base thickness, leading to less fatigue damage. However, throughout the design space, there are many local minima and many regions where fatigue constraints are not satisfied. These include the regions shown in red in figure 5, where the damage over 1 second exceeds 1%. Furthermore, transitions between regions of low and high damage are not necessarily smooth, suggesting that for these problems a local optimization strategy was unlikely to find a global optimum and that a global optimization approach would be necessary.

3.3. Optimisation study

This section explores the optimal thickness design of a configuration comprising of two notched plates attached to a flexible beam. The excitation location and the boundary conditions used are indicated in figure 6. Both plates are subjected to the point loads located in their respective outboard corners. To allow for greater design variation, the plates were divided into 10 different zones whose thicknesses could be varied. In order to investigate whether different spectral loads resulted in different recommended thickness distributions, the test case was optimised using a PSD defined in 3 different frequency ranges. To ensure that the 9th mode at 61.5 Hz was included, the chosen ranges were 0-21 Hz, 21-42 Hz and 42-63 Hz. A simulation with excitation specified over the entire 0-63 Hz range was also performed.

During optimisation, the thicknesses were allowed to vary according to the chosen problem parameterisation. However, a localised plate thinning or thickening could change the stiffness such that the modes of interest would exit or reenter the defined frequency envelope. To address this issue, while excitation was only considered in the range up to 63 Hz to excite the first 33 modes, the modal analysis was directed to include the first 70 vibration modes. This approach ensured that the modal fluctuations resulting from the thickness variations were correctly captured during optimisation.

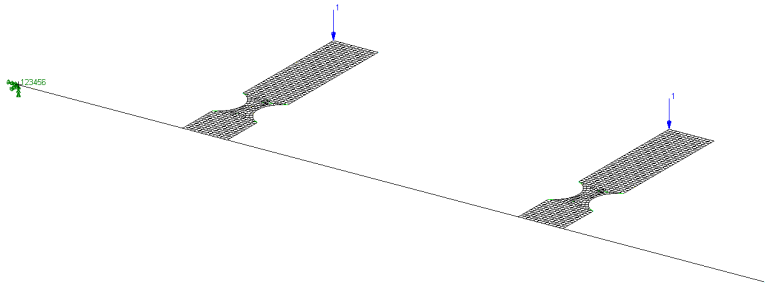

Figure 6: FE model of the fully assembled beam structure with two nominally identical notched plates

Figure 7 shows an example of a constrained optimization (see section 2.4.) which succeeded in achieving a 47.9% weight reduction compared to a design based on having a uniform thickness. The log of fatigue damage for the uniform thickness example is shown on the left. The variable thickness design's damage is shown in the centre, and its thickness distribution is shown on the right. The figure makes it clear that the highest fatigue damage is concentrated at the base of the lightweight structure and in the notch region of the right-hand plate for the uniform thickness sample. Hence, much of the structure has a longer fatigue life than is necessary and is overly heavy. By contrast, the optimized variable thickness design shows a similar level of damage throughout the structure.

Several characteristics of the optimized design are notable. Firstly, mass can be decreased by varying the plate thickness across the parameterised regions. Specifically, the thicker side tends to alternate between the left and right side in each parameterised pair located in the plates' spanwise direction. The optimiser has converged towards what is close to a checkerboard pattern. While this does save weight, it can also be a result of numerical artifacts which aritficially raise stiffness.

It is thought that this solution is influenced by a combination of the asymmetric load placement, activated torsional modes as well as the variable elastic coupling originating from the particular distribution of the plates across the beam. As expected, some of the thickest regions are at the base and at the notch. This is in line with previously discussed damage plots. Additionally, in contrast with the uniform thickness

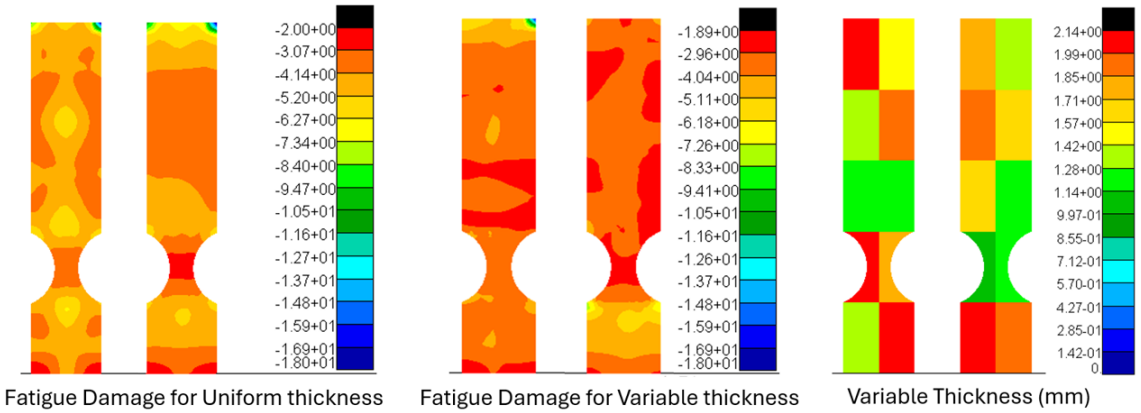

Figure 7: Excitation in range 0-63 Hz. Log of fatigue damage for coupled plates optimised with uniform thickness (left), and initially varied thickness (centre) are shown. The thickness distribution used to generate the central figure is shown (right).

cases, the regions near the top left-hand corners have also increased thickness. As that is where the point loads are applied, this result represents a rational design solution. Overall, the recommended design, with an average thickness of 1.61 mm, is significantly lighter than the design optimised with a uniform thickness (2.95 mm) and the reference design (3 mm) and can be considered highly conditional to the loading (both in the spatial and spectral sense) as well as the plate placement context on the flexible support structure.

Figure 8 shows resulting thickness distributions obtained using optimisation with different PSD excitation frequency ranges. From left to right, these are 0-21 Hz, 21-42 Hz, 42-63 Hz and previously discussed 0-63 Hz range. While the 0-21 Hz and 0-63 Hz spectrums resulted in designs with a 24.9 % and 45.7% weight saving compared to the design with a uniform thickness, the designs obtained for the 21-42 Hz and the 42-63 Hz ranges were 0.7% and 0.5% heavier than their uniform thickness alternatives, respectively. In these cases, the optimization procedure was not able to achieve improved mass-based design. This suggests that the loading frequency content and its relationship with the spectral distribution of the vibration modes is a decisive factor in successful application of this methodology. Overall, the optimized designs in figure 8 show similarities in converging on checkerboard-type thickness distribution and thick choices at their notches.

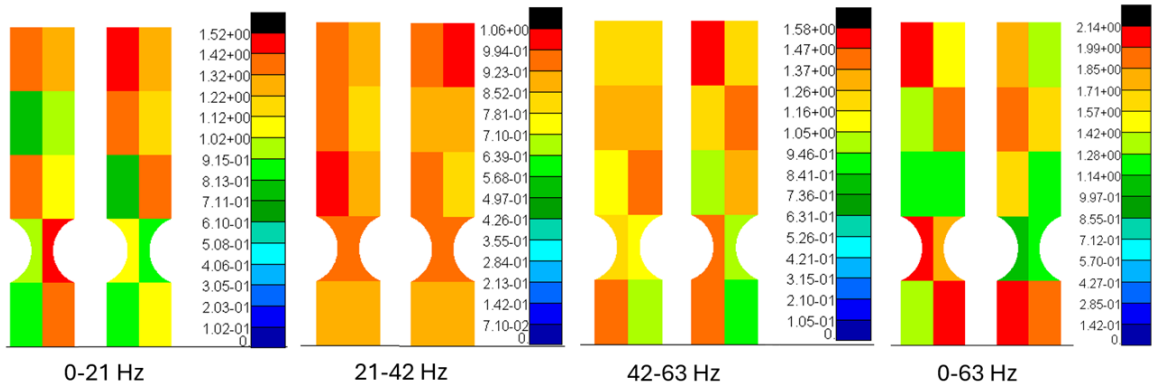

Figure 8: Optimized thickness distributions in mm for different excitation frequency ranges.

4. DISCUSSION

The investigation into the optimisation for fatigue of lightweight structures has produced several interesting findings. First, the initial modal analysis revealed that notched plates provide a good test case

to evaluate optimal thickness design analysis since maximum stresses occur in multiple regions. It also showed that a coupled system of two plates attached to a beam creates a significantly more complex system, with 33 modes required to capture the 9th mode observed in an isolated notched plate.

Next, optimisation studies were performed by varying the thickness parameters assigned to the selected plate regions while satisfying fatigue damage constraints. An initial optimisation was performed where the plate thickness was kept uniform, resulting in an optimised design that still maintained a uniform thickness. Then, a locally parameterised optimisation with multiple restarts was completed, allowing for many different initial thickness distributions.

In cases where excitation activated modes in a low-frequency range (0-21 Hz), the optimisation of provided several configurations which performed better than uniform thickness distributions. These included several features which would not be immediately apparent to designers. These principally included a checkerboard-type pattern of alternating thickness, a strong base and notched section, and a thickening of the plates near where the load is applied. Of these features, the checkerboard pattern should be treated with caution. Checkerboard patterns can emerge naturally as a vibration reducing feature, as they do, for example, from topological, cellular automata and combinatorial optimisation techniques used in viscoelastic damping technologies [17][18][19]. However, checkerboarding can also be the result of numerical artifacts, which can cause overestimated stiffness. In this case, thicknesses never fall to zero, as is the case with an obvious checkerboard artifact. However, the alternating pattern is not consistent across the top 5% of designs, and further work is being done to identify whether a more consistent pattern can be arrived at. In cases where excitation was concentrated at higher frequencies, varied thickness distributions did not provide lighter overall designs compared to uniform thickness optimisations. This is an important finding with clear implications for complex and industrially-relevant applications. There are several possible explanations for this. These simulations may have been limited by the relatively large size of the parameterised regions used. Since mode shapes at higher frequencies have shorter typical wavelengths, a plate that is only divided into five sections spanwise and two across its width provides a mesh that is too coarse to allow effective optimisation. It may also be the case that superior designs exist and that using 400 restarts was insufficient to identify them. Further work with finer design meshes and more robust global optimisation strategies will be necessary.

Having made allowances for these limitations, for applications where low-frequency excitation forms a significant part of the system loading, the optimal search approach can provide significant design improvements. Using a Latin hypercube remains a relatively crude global optimisation technique. In problems with many design variables, more optimal designs are likely to be missed unless very large numbers of samples are used. This motivates future work, which will seek to improve on this method with dedicated global optimisation strategies such as agent-based modelling.

5. CONCLUSIONS

The project has achieved its aim to demonstrate the benefits of an optimal design methodology which accounts for the fatigue damage factors in the context of lightweight components attached to flexible support structures. By evaluating the fatigue damage using the Dirlik method and formulating an optimization setup with the IPOPT algorithm, which allowed for variation of the regional thicknesses, notable improvements in the component weight were obtained under the fatigue damage constraints.

An improved understanding of the design space which such problems present has been obtained, revealing, in particular, the highly non-smooth design space which such fatigue optimisation studies must contend with. Further work will consist of evaluating simulations with refined and smaller parameterised regions, the use of more complex excitation spectra informed by the real flight conditions, as well as implementing a dedicated global optimization algorithm, such as using agent-based modelling. The future models will be subjected to in-flight PSD excitation data rather than simple synthetic excitation spectra. These tasks will also be tied to more complex component geometries relevant to specific lightweight wing structures instead of the flat plates used in this study.

ACKNOWLEDGMENTS

This work was supported by the Aerospace Technology Institute and Innovate UK through the Out of Cycle NExt Generation Highly Efficient Air Transport (ONEheart) project - grant number 10003388. The authors gratefully acknowledge the support that Francesco Gambioli and Dirk Pantone have provided to this work.

REFERENCES

[1] A. Palmgren. Die lebensdauer von kugellagern. *Zeitschrift des Vereins Deutscher Ingenieure*, 68 (14):339–341, 1924.

[2] M. A. Miner. Cumulative damage in fatigue. *Journal of Applied Mechanics*, 12(3):A159–A164, 1945.

[3] Masanori Matsuishi and Tatsuo Endo. Fatigue of metals subjected to varying stress. *Japan Society of Mechanical Engineers*, 68(2):37–40, 1968.

[4] John W. Miles. On structural fatigue under random loading. *Journal of the Aeronautical Sciences*, 21(11):753–762, 1954.

[5] Turan Dirlik. *Application of Computers in Fatigue Analysis*. PhD thesis, University of Warwick, 1985. URL https://api.semanticscholar.org/CorpusID:108432882.

[6] Yeh-Liang Hsu and Ming-Sho Hsu. Weight reduction of aluminum disc wheels under fatigue constraints using a sequential neural network approximation method. *Computers in Industry*, 46 (2):167–179, 2001.

[7] M Mrzyglod and AP Zielinski. Parametric structural optimization with respect to the multiaxial high-cycle fatigue criterion. *Structural and multidisciplinary optimization*, 33:161–171, 2007.

[8] Necmettin Kaya, Idris Karen, and Ferruh Öztürk. Re-design of a failed clutch fork using topology and shape optimisation by the response surface method. *Materials & Design*, 31(6):3008–3014, 2010.

[9] Ding Peng Liu, Giulio Ferri, Taemin Heo, Enzo Marino, and Lance Manuel. On long-term fatigue damage estimation for a floating offshore wind turbine using a surrogate model. *Renewable Energy*, 225:120238, 2024. ISSN 0960-1481. doi: https://doi.org/10.1016/j.renene.2024.120238. URL https://www.sciencedirect.com/science/article/pii/S0960148124003033.

[10] Aleksandar Grbović, Gordana Kastratović, Aleksandar Sedmak, Khalid Eldweib, and Snezana Kirin. Determination of optimum wing spar cross section for maximum fatigue life. *International Journal of Fatigue*, 127:305–311, 2019. ISSN 0142-1123. doi: https://doi.org/10.1016/j.ijfatigue.2019.06.019. URL https://www.sciencedirect.com/science/article/pii/S0142112319302488.

[11] J.R. Wright and J.E. Cooper. *Introduction to Aircraft Aeroelasicity and Loads*. Wiley, Chichester, UK, 2015.

[12] Hexagon. CAE Fatigue Frequency package. https://hexagon.com/products/caefatigue-frequency-package. Accessed: 23 Feb. 2025.

[13] The Engineering Lab. Sol 200 web app. URL https://the-engineering-lab.com/.

[14] Aluminum Company of America. *Alcoa Structural Handbook: A Design Manual for Aluminum*. Aluminum Company of America, Pittsburgh, Pa., revised ed. edition, 1960. URL https://catalog.hathitrust.org/Record/009850859.

[15] Andreas Wächter and Lorenz T. Biegler. On the implementation of an interior-point filter line-search algorithm for large-scale nonlinear programming. *Mathematical Programming*, 106(1):25–57, Mar 2006.

[16] Janko Slavič, Matjaž Mršnik, Martin Česnik, Jaka Javh, and Miha Boltežar. Chapter 6 - vibration fatigue analysis using modal decomposition. In Janko Slavič, Matjaž Mršnik, Martin Česnik, Jaka Javh, and Miha Boltežar, editors, *Vibration Fatigue by Spectral Methods*, pages 127–134. Elsevier, 2021. ISBN 978-0-12-822190-7. doi: https://doi.org/10.1016/B978-0-12-822190-7.00013-X. URL https://www.sciencedirect.com/science/article/pii/B978012822190700013X.

[17] C M Chia, J A Rongong, and K Worden. Evolution of constrained layer damping using a cellular automaton algorithm. *Proceedings of the Institution of Mechanical Engineers, Part C*, 222(4):585–597, 2008. doi: 10.1243/09544062JMES638.

[18] Francesca Curà, Andrea Mura, and Fabrizio Scarpa. Modal strain energy based methods for the analysis of complex patterned free layer damped plates. *Journal of Vibration and Control*, 18(9):1291–1302, 2012. doi: 10.1177/1077546311417277.

[19] G. Delgado and M. Hamdaoui. Topology optimization of frequency dependent viscoelastic structures via a level-set method. *Applied Mathematics and Computation*, 347:522–541, 2019. ISSN 0096-3003. doi: https://doi.org/10.1016/j.amc.2018.11.014. URL https://www.sciencedirect.com/science/article/pii/S0096300318309871.